

SINGLE-WALLED CARBON NANOTUBE-BASED HYBRID MATERIALS FOR MANAGING CHARGE TRANSFER PROCESSES

Theodoros A. Felekis and Nikos Tagmatarchis

National Hellenic Research Foundation, Theoretical and Physical Chemistry Institute, Vass. Constantinou 48 Ave., Athens 116 35, Greece

Received: April 26, 2005

Abstract. Functionalized single-walled carbon nanotubes possessing photoactive units have been prepared, analytically characterized and morphologically visualized. The characteristic electron donor has been realized either by covalent attachment onto the sidewalls of SWNTs or alternatively by supramolecular van-der-Waals / electrostatic interactions giving rise to diverse hybrid systems. Intramolecular electron transfer processes within these nanohybrids were probed by fluorescence and transient absorption spectroscopy.

1. INTRODUCTION

Due to extraordinary electronic, physicochemical and mechanical properties carbon nanotubes (CNT) represent an attractive building block for the realization of numerous nanotechnological applications [1,2]. Lately, the prospect for developing novel devices based on CNT materials for optoelectronics, molecular electronics and plastic solar cells has excited worldwide scientific interest. However, CNT applications development is challenged by several issues such as $\pi-\pi$ stacking interactions between individual tubes resulting in the formation of bundles of CNT with different length, diameter and chirality, defect sites around the CNT skeleton and insolubility. All these parameters bring difficulties on manufacturing CNT while manipulation and full characterization set back.

Chemical functionalization of CNT appeared as a powerful tool to overcome some of these problems by giving the desired solubility. During the last five years several methods were developed for the functionalization of the ends or the sidewalls of CNT as nicely presented in several review articles [3-9].

Certain role among the functionalization techniques plays the 1,3-dipolar cycloaddition of azomethine ylides onto the sidewalls of CNT [10-13]. The applicability of the method relies on the fact that utilizes commercially available or easily achievable by simple synthetic steps, aldehydes and α -aminoacids. Furthermore, not only solubility of the so-functionalized CNT is obtained in organic solvents but also nanohybrids consisting of CNT and organic moieties carrying characteristic units suitable for projected applications are formed.

Herein, we present diverse approaches towards the formation of nanohybrids consisting of single-walled carbon nanotube (SWNT) units and electron-donor moieties such as porphyrinic and ferrocenyl units *en route* to versatile donor-acceptor nanosized ensembles for managing photoinduced electron transfer processes.

2. EXPERIMENTAL SECTION

The SWNT used in these studies were produced by Carbon Nanotechnologies Inc., by the HiPco process (<http://cnanotech.com>) and purified under

Corresponding author: Nikos Tagmatarchis, e-mail: tagmatar@eie.gr

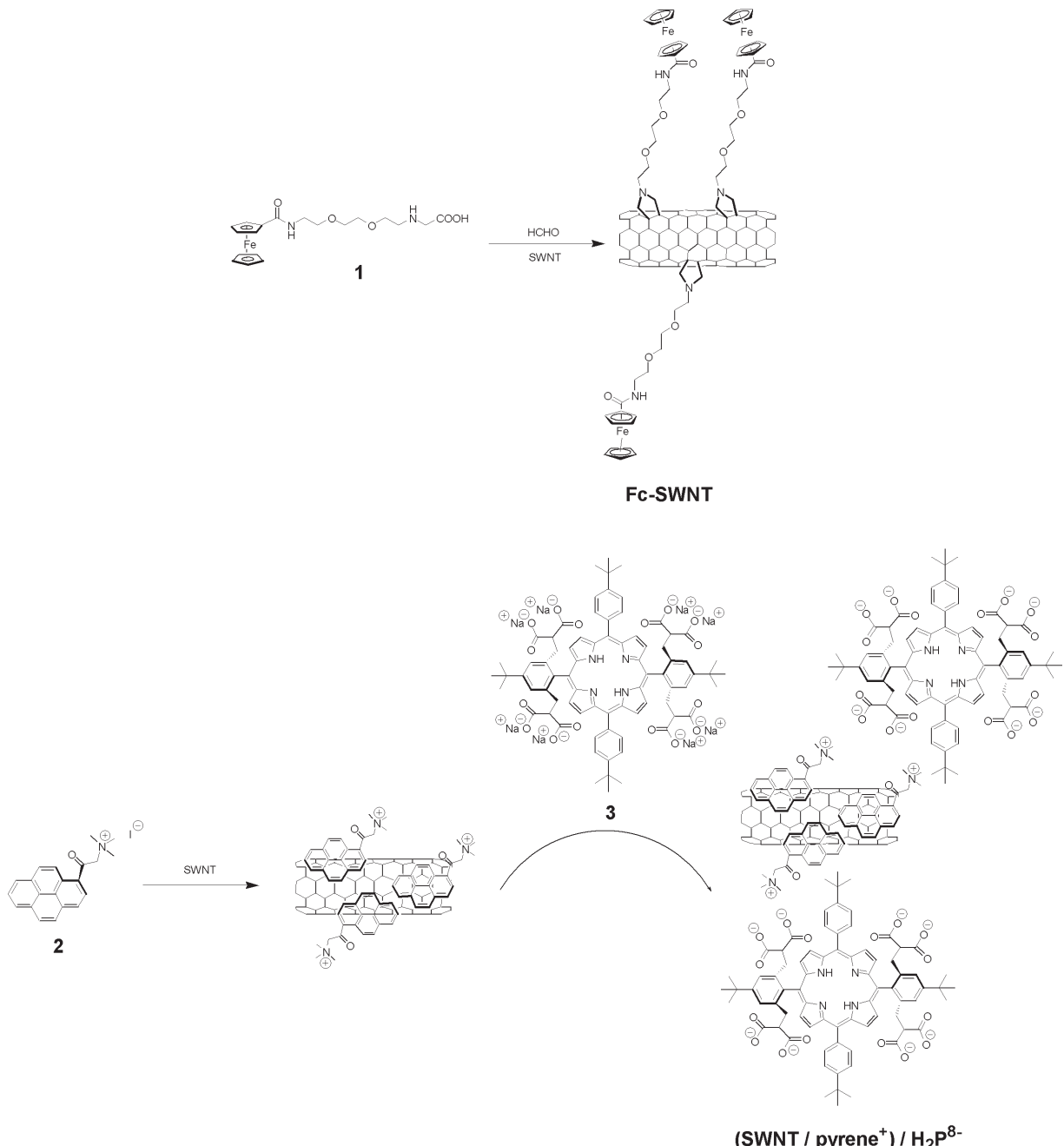


Fig. 1. Synthesis of (a) **SWNT-Fc** and (b) **(SWNT·pyrene⁺)·H₂P⁸⁻** nanoensembles.

acidic and thermal treatment to remove metal nanoparticles. Ferrocene modified glycine **1** and paraformaldehyde together with SWNT suspended in DMF were heated to 130 °C for 96 hours. After that period the solvent was evaporated and the desired material **SWNT-Fc** was isolated following our published procedure. On the other hand, mixing and sonicating purified HiPco SWNT with a concentrated aqueous solution of the positively charged pyrene derivative **2** results in a stable suspension of **SWNT·pyrene⁺** complex. Addition of 10 wt. % of

the corresponding porphyrin **3** favors the electrostatic formation of the nanoensemble **(SWNT·pyrene⁺)·H₂P⁸⁻**.

3. DISCUSSION

SWNT were covalently functionalized by the powerful methodology of 1,3-dipolar cycloaddition of azomethine ylides generated *in-situ* by the thermal condensation of a ferrocene modified glycine **1** and paraformaldehyde (Fig. 1a). With this methodologi-

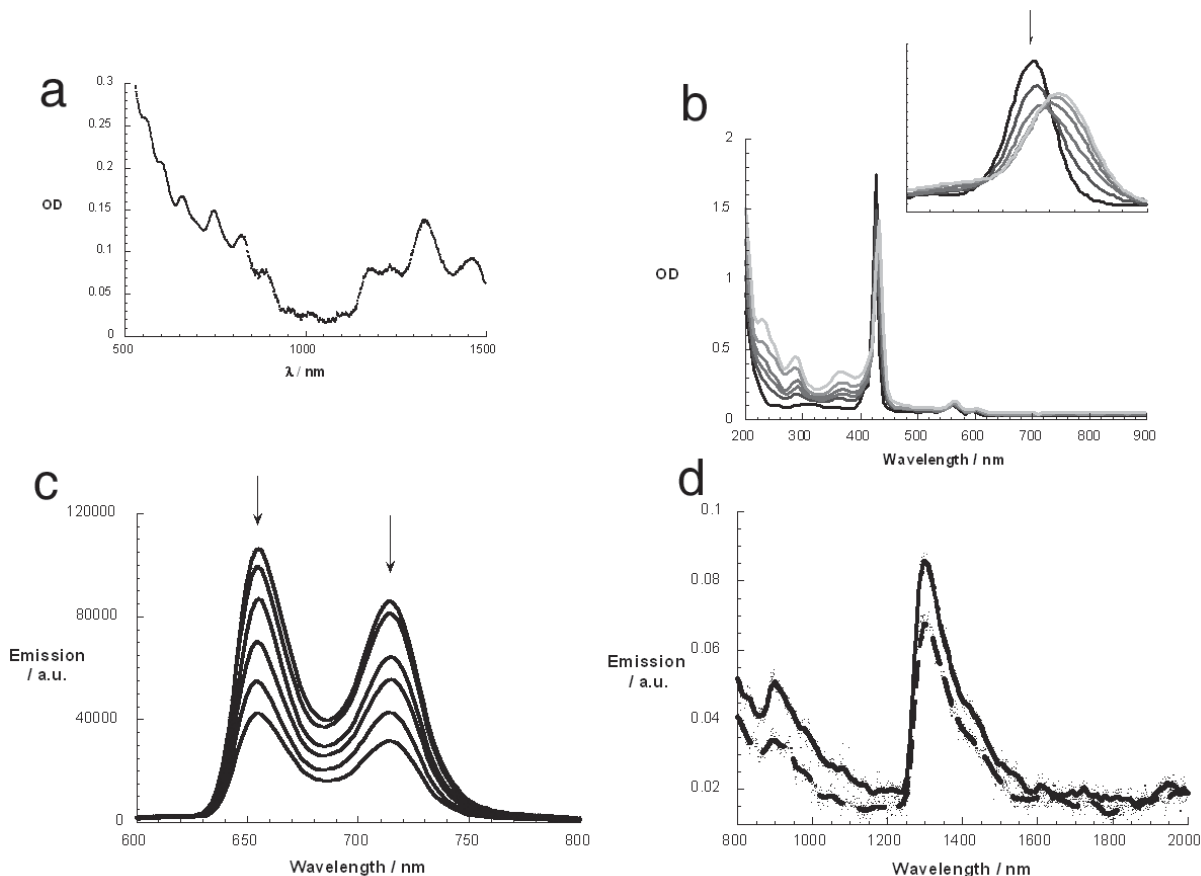


Fig. 2. Electronic absorption spectra of (a) **SWNT·pyrene⁺** showing the characteristic van Hove singularities corresponding to the S_{11} , S_{22} and M_{11} semiconducting and metallic SWNT and (b) **(SWNT·pyrene⁺)·H₂P⁸⁻** showing the characteristic Soret- and Q- band transitions red-shifted (see inset). Fluorescence emission spectra of (c) **(SWNT·pyrene⁺)·H₂P⁸⁻** as formed upon titrating H_2P^{8-} with several concentrations of **SWNT·pyrene⁺** following excitation at 430 nm (arrows indicate quenching) and (d) **SWNT-Fc** (dashed line) and **SWNT-TEG** (solid line) following excitation at 355 nm.

cal approach a plethora of pyrrolidine units and thus, of ferrocenyl groups as a linear extension from the fused pyrrolidine ring, were covalently introduced onto the side walls of SWNT, giving rise to highly soluble material, namely **SWNT-Fc** [14-16]. The electronic absorption spectrum of **SWNT-Fc** recorded in dichloromethane solution is featureless while its intensity monotonically decreases as reaches the NIR region. The fusion of every pyrrolidine ring onto the sidewalls of CNT requires the loss of two electrons from the highly conjugated network of SWNT. The presence of metallic and semiconducting electronic transitions are missing due to the disruption of the continuous π -network system and the introduction of an increased amount of defects (sp^3 sites where the pyrrolidine rings are fused onto the SWNT skeleton upon functionalization), are indicative of dramatic changes in the novel electronic properties of SWNT.

With an eye to keep intact the novel electronic properties of SWNT, nanotube-based donor-acceptor nanoensembles were realized by supramolecular means. In this context, SWNT were first brought into solution by non-covalent interactions with a positively charged pyrene derivative (**2**), namely **pyrene⁺**, and then electrostatically coupled to the donor moiety (**3**) - a negatively charged porphyrin (**3**), namely **H₂P⁸⁻** [17]. Thus, in the electronic absorption spectrum of **SWNT·pyrene⁺** (Fig. 2a) the characteristic van Hove singularities corresponding to the S_{11} , S_{22} and M_{11} semiconducting and metallic SWNT [18-21], respectively, are easily discernable. Furthermore, the strong $\pi-\pi$ transitions of **pyrene⁺** can be found slightly red-shifted in the

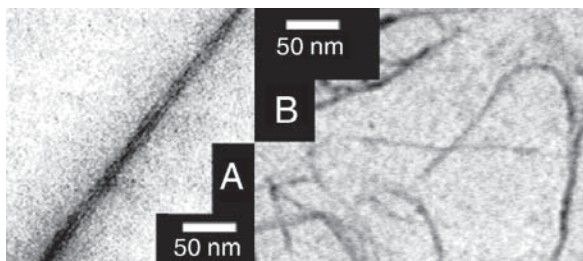


Fig. 3. Transmission electron micrographs of (a) **SWNT-Fc**, and (b) **(SWNT·pyrene⁺)·H₂P⁸⁻** nanohybrids, respectively.

UV-Vis region of the spectrum, as compared with the starting compound **2**. The latter observation stresses the electronic communication between the two systems while the former gives strong evidence that the novel electronic properties of SWNT remained virtually unchanged upon the van-der-Waals complexation of the **pyrene⁺** derivative.

Having preserved the electronic properties of SWNT upon van-der-Waals-complexation of SWNT with **pyrene⁺**, the octaanionic porphyrin **3** is anchored to the positively charged trimethylammonium groups of the **SWNT·pyrene⁺** supramolecular complex to furnish the **(SWNT·pyrene⁺)·H₂P⁸⁻** nanoensemble (Fig. 1b). When dilute aqueous solutions of **H₂P⁸⁻** titrated with variable amounts of **SWNT·pyrene⁺** several changes in both the absorption and fluorescence spectra observed. In the absorption spectrum, the characteristic Soret- and Q-band transitions are red-shifted while the $\pi-\pi$ transitions of **pyrene⁺** are furthermore red-shifted (Fig. 2b). The former indicates the change that occurs in the **H₂P⁸⁻** (upon titration with **SWNT·pyrene⁺**) while the latter observation is evidence of interactions and the electronic communication that occurs between **SWNT·pyrene⁺** and **H₂P⁸⁻**. The strong fluorescence emission at 655 nm and 715 nm of photoexcited **H₂P⁸⁻** is quenched upon addition of **SWNT·pyrene⁺** (Fig. 2c). The decrease is exponential and depends solely on the concentration of the added **SWNT·pyrene⁺**. For the fluorescence profiles lifetimes of 2.1 ns and 0.2 ns respectively were determined. As the concentration of **SWNT·pyrene⁺** increases the contribution of the short-lived component increases as well.

The electron-transfer interactions in the photoexcited states of SWNT were probed by fluorescence and transient absorption spectroscopy experiments. As shown in Fig. 2d, quenching of fluorescence in **SWNT-Fc** nanohybrids, relative to the

one taken from a reference material where the amidoferrocenyl units were replaced by methoxy ones (namely TEG-SWNT), was observed. Further support for quenching of the electron transfer from the photoexcited ferrocene unit to the SWNT ground state comes from transient absorption spectroscopy where careful analysis of the decay component of **(Fc)⁺ – (SWNT)⁰** yields a lifetime of 1100 ± 100 ns. In addition, bulk electrolysis and pulse radiolysis experiments verified the formation of reduced SWNT in **(Fc)⁺ – (SWNT)⁰**, by showing a UV-Vis-NIR spectrum virtually identical to the transient one obtained.

At this point it should be mentioned that when only **pyrene⁺** was used for the titration experiments, instead of the supramolecular complex **SWNT·pyrene⁺**, the before-mentioned observations and electronic shifts were not observed in the same extent. This means that the presence of SWNT in the form of **SWNT·pyrene⁺** complex augments the electronic perturbation of the π -system of the porphyrin. In addition, interactions of **SWNT·pyrene⁺** complex with an oligocationic porphyrin were studied. To this end, zinc 5,10,15,20-tetrakis-(2',6'-bis(N-methylene- (4"-tert-butylpyridinium))-4'-tert-butylphenyl) porphyrin octabromide (**ZnP⁸⁺**) was used. However, due to repulsive interactions both the electronic absorption and fluorescence spectra remained throughout the titration experiments virtually unchanged.

Finally, transmission electron microscopy (TEM) verified the presence of SWNTs in the above mentioned nanoensembles. The micrograph of **SWNT-Fc** is shown in Fig. 3a. For the TEM deposition diethyl ether was used as a solvent in which the examined nanohybrids are suspended, and thus, can be easily visualized under the microscope, forming thin bundles. As long as the van-der-Waals / electrostatically interacting **(SWNT·pyrene⁺)·H₂P⁸⁻** nanoensemble concerns, bundles of nanotubes with diameter of less than 20 nm and lengths of several micrometers are seen in Fig. 3b. Furthermore, darker areas surrounding the SWNT skeleton may be attributed to the presence of the octaanionic porphyrin **H₂P⁸⁻** electrostatically interacting with the **(SWNT·pyrene⁺)** supramolecular complex.

4. CONCLUSIONS

SWNT-based nanohybrids have been realized where the nanotube part serves as the electron acceptor unit and ferrocene covalently attached through a flexible pyrrolidine-oligoethylene chain onto the sidewalls of SWNT serves as the photoexcited electron acceptor. Alternatively, an oligoanionic porphy-

rin moiety as the photoexcited electron donor was electrostatically coupled to a **SWNT·pyrene⁺** complex. Results based on fluorescence and transient absorption spectroscopy verified the electron transfer interactions and opens the way for the construction of novel nanosized architectures for managing such processes.

ACKNOWLEDGEMENTS

Part of the presented work was financially supported by EUROHORCs/ESF through the European Young Investigator (EURYI-2004) Awards Scheme.

REFERENCES

- [1] P. Harris, *Carbon Nanotubes and Related Structures: New Materials for the Twenty-First Century* (Cambridge University Press, Cambridge, 2001).
- [2] S. Reich, C. Thomsen and J. Maultzsch, *Carbon Nanotubes: Basic Concepts and Physical Properties* (Wiley-VCH, Weinheim, 2004).
- [3] A. Hirsch // *Angew. Chem. Int. Ed.* **41** (2002) 1853.
- [4] J. L. Bahr and J. M. Tour // *J. Mater. Chem.* **12** (2002) 1952.
- [5] S. Niyogi, M. A. Hamon, H. Hu, B. Zhao, P. Bhowmik, R. Sen, M. E. Itkis and R. C. Haddon // *Acc. Chem. Res.* **35** (2002) 1105.
- [6] Y.-P. Sun, K. Fu, Y. Lin and W. Huang // *Acc. Chem. Res.* **35** (2002) 1096.
- [7] D. Tasis, N. Tagmatarchis, V. Georgakilas and M. Prato // *Chem. Eur. J.* **9** (2003) 4000.
- [8] S. Banerjee, M. G. C. Kahn and S. S. Wang // *Chem. Eur. J.* **9** (2003) 1898.
- [9] C. A. Dyke and J. M. Tour // *Chem. Eur. J.* **10** (2004) 812.
- [10] V. Georgakilas, K. Kordatos, M. Prato, D. M. Guldi, M. Holzinger and A. Hirsch // *J. Am. Chem. Soc.* **124** (2002) 760.
- [11] V. Georgakilas, N. Tagmatarchis, D. Pantarotto, A. Bianco, J.-P. Briand and M. Prato // *Chem. Commun.* (2002) 3050.
- [12] N. Tagmatarchis and M. Prato // *J. Mater. Chem.* **14** (2004) 437.
- [13] D. Pantarotto, C. D. Partidos, R. Graff, J. Hoebeke, J. -P. Briand, M. Prato and A. Bianco // *J. Am. Chem. Soc.* **125** (2003) 6160.
- [14] D. M. Guldi, M. Marcaccio, D. Paolucci, F. Paolucci, N. Tagmatarchis, D. Tasis, E. Vazquez and M. Prato // *Angew. Chem. Int. Ed.* **42** (2003) 4206.
- [15] A. Callegari, M. Marcaccio, D. Paolucci, F. Paolucci, N. Tagmatarchis, D. Tasis, E. Vazquez and M. Prato // *Chem. Commun.* (2003) 2576.
- [16] A. Callegari, S. Cosnier, M. Marcaccio, D. Paolucci, F. Paolucci, V. Georgakilas, N. Tagmatarchis, E. Vazquez and M. Prato // *J. Mater. Chem.* **14** (2004) 807.
- [17] D. M. Guldi, G. M. A. Rahman, N. Jux, N. Tagmatarchis and M. Prato // *Angew. Chem. Int. Ed.* **43** (2004) 5526.
- [18] M. S. Strano, C. B. Huffman, V. C. Moore, M. J. O'Connell, E. H. Haroz, J. Hubbard, M. Miller, K. Rialon, C. Kittrell, S. Ramesh, R. H. Hauge and R. E. Smalley // *J. Phys. Chem. B* **107** (2003) 6979.
- [19] W. Zhao, C. H. Song and P. E. Pehrsson // *J. Am. Chem. Soc.* **124** (2002) 12418.
- [20] S. Kazaoui, N. Minami, N. Matsuda, H. Kataura and Y. Achiba // *Appl. Phys. Lett.* **78** (2001) 3433.
- [21] S. Kazaoui, N. Minami, R. Jacquemin, H. Kataura and Y. Achiba // *Phys. Rev. B* **60** (1999) 13339.